Brain Struct Funct (2017) 222:3127–3145
DOI 10.1007/s00429-017-1390-6

ORIGINAL ARTICLE

Top-down cortical interactions in visuospatial attention

Timothy P. Meehan[1] · Steven L. Bressler[1,2] · Wei Tang[1] · Serguei V. Astafiev[3] · Chad M. Sylvester[4] · Gordon L. Shulman[5] · Maurizio Corbetta[3,5,6]

Received: 5 February 2016 / Accepted: 23 February 2017 / Published online: 20 March 2017

Abstract The voluntary allocation of visuospatial attention depends upon top-down influences from the frontal eye field (FEF) and intraparietal sulcus (IPS)—the core regions of the dorsal attention network (DAN)—to visual occipital cortex (VOC), and has been further associated with within-DAN influences, particularly from the FEF to IPS. However, the degree to which these influences manifest at rest and are then modulated during anticipatory visuospatial attention tasks remains poorly understood. Here, we measured both undirected and directed functional connectivity (UFC, DFC) between the FEF, IPS, and VOC at rest and during an anticipatory visuospatial attention task, using a slow event-related design. Whereas the comparison between rest and task indicated FC modulations that persisted throughout the task duration, the large number of task trials we collected further enabled us to measure shorter timescale modulations of FC across the trial. Relative to rest, task engagement induced enhancement of both top-down influences from the DAN to VOC, as well as bidirectional influences between the FEF and IPS. These results suggest that task performance induces enhanced interaction within the DAN and a greater top-down influence on VOC. While resting FC generally showed right hemisphere dominance, task-related enhancement favored the left hemisphere, effectively balancing a resting hemispheric asymmetry, particularly within the DAN. On a shorter (within-trial) timescale, VOC-to-DAN and bidirectional FEF-IPS influences were transiently elevated during the anticipatory period of the trial, evincing phasic modulations related to changing attentional demands. In contrast to these task-specific effects, resting and task-related influence patterns were highly correlated, suggesting a predisposing role for resting organization, which requires minimal tonic and phasic modulations for control of visuospatial attention.

Keywords Dorsal attention network · Hemispheric asymmetry · Intrinsic connectivity · Task set · Cognitive control

Electronic supplementary material The online version of this article (doi:10.1007/s00429-017-1390-6) contains supplementary material, which is available to authorized users.

✉ Steven L. Bressler
bressler@fau.edu

[1] Center for Complex Systems and Brain Sciences, Florida Atlantic University, 777 Glades Road, Boca Raton, FL 33431, USA

[2] Department of Psychology, Florida Atlantic University, Boca Raton, FL 33431, USA

[3] Department of Radiology, Washington University School of Medicine, St. Louis, MO 63110, USA

[4] Department of Psychiatry, Washington University School of Medicine, St. Louis, MO 63110, USA

[5] Department of Neurology, Washington University School of Medicine, St. Louis, MO 63110, USA

[6] Department of Neurobiology, Washington University School of Medicine, St. Louis, MO 63110, USA

Introduction

The dorsal attention network (DAN), a bilateral system of frontal and parietal regions anchored on the frontal eye fields (FEF) and intraparietal sulci (IPS), has been proposed to facilitate voluntary orienting of visuospatial attention by exerting top-down influence on visual occipital cortex (VOC) (Corbetta and Shulman 2002). During anticipatory attention, in which an observer utilizes

advance information to orient to the location of an impending visual target, this top-down influence is thought to drive stimulus-independent, endogenous visual cortical activity (Kastner et al. 1999; Hopfinger et al. 2000; Silver et al. 2007; Sylvester et al. 2007), which in turn likely underlies superior detection upon the target's appearance (Eriksen and Hoffman 1972; Posner 1980; Carrasco 2011). Evidence supporting this mechanism has come via intracranial microstimulation of DAN regions in monkeys (Moore and Armstrong 2003a; Moore and Fallah 2004) and transcranial magnetic stimulation in humans (Ruff et al. 2006; Capotosto et al. 2009, 2012; Marshall et al. 2015), as well as without intervention via causal modeling of fMRI-BOLD signal time series from DAN and VOC regions in humans (Bressler et al. 2008; Vossel et al. 2012). In addition, several studies have reported that, within the DAN itself, frontoparietal coupling and/or directed influences increase during voluntary visual orienting (Buschman and Miller 2007; Bressler et al. 2008; Ozaki 2011; Vossel et al. 2012) or visuospatial judgment (De Graaf et al. 2009, 2010). Altogether, this evidence points to an influence pattern consisting of both elevated frontoparietal interaction and top-down DAN→VOC modulation as crucial for the control of visuospatial attention.

Because prior evidence was derived largely from studies where influences were explicitly induced by stimulation and/or task demands, the extent to which these influences depart from resting organization has remained underexplored. One possibility is that task-related influences supporting top-down attention represent a profound reconfiguration of resting organization, while an alternative is that resting influences provide a framework for those underlying task execution. Favoring the latter, several studies have shown the spontaneous activity of task-related networks to be relevant to both task-related activity (Fox et al. 2006) and behavior (He et al. 2007; Fox et al. 2007; Sadaghiani et al. 2010; Baldassarre et al. 2012, 2014). Additionally, more recent studies have shown that task engagement largely modulates rather than reconfigures intrinsic organization, resulting in close correspondence of resting and task-related connectivity patterns (Cole et al. 2014; Spadone et al. 2015). However, an outstanding question remains as to whether the modulations underlying top-down attention occur mainly on a long timescale that spans the duration of a task, or whether further modulations occur on a shorter (within-trial) timescale. Because resting organization may indicate the presence of strong intrinsic constraints on task-related network interactions, a better understanding of the dynamics of its modulation is paramount for understanding the network basis for top-down attention.

Previously, we showed that top-down DAN→VOC and FEF→IPS influences predominate at the moment directly preceding the appearance of an anticipated visual stimulus during an anticipatory visual attention task (Bressler et al. 2008), but did not determine whether and to what extent these influences depart from resting organization or change across the trial. Thus, here we utilized this existing dataset (Sylvester et al. 2007) and complemented it with resting data collected subsequently from a separate group of subjects whose resting activity would not reflect any learning effects from task training or performance. To assess the task-related modulation of resting influences occurring both between the DAN and VOC, and within the DAN, we measured directed functional connectivity (DFC) using multivariate vector autoregressive (MVAR) analysis of fMRI-BOLD time series recorded from both groups of subjects. Whereas similarities between task and resting DFC suggested that pre-existing resting influence patterns shape task-related patterns, task-rest differences suggested that resting patterns are reconfigured by anticipatory attention. Furthermore, to assess shorter (within-trial) timescale modulations, we compared DFC patterns from the anticipatory delay period of the trial to those from the rest-like inter-trial interval (ITI). This was made possible by the slow event-related design and the large number of task trials collected, which is critical for accurate MVAR estimation at each trial time point. Finally, because functional connectivity studies have typically employed correlation-based undirected functional connectivity (UFC), we also compared UFC with DFC patterns to judge the relative utility of DFC and UFC measures. Our results suggest that resting influence patterns shape task-induced influences, with subtle reconfiguration of resting organization on both long and short timescales subserving the control of visuospatial attention.

Materials and methods

Participants and task

Six right-handed subjects (three male, three female), aged 26–30, performed a demanding visual spatial attention task as previously described (Sylvester et al. 2007) (Fig. 1). Each subject in this Task Group performed 500–900 task trials, requiring a large total task performance time (8–12 scanning sessions per subject). An additional twenty-three subjects, aged 22–35 (eight male, fifteen female), were included in the study as a Rest Group. These subjects had no experience in the visual spatial attention task. They were instructed to lie still in the scanner and fixate their gaze on a central crosshair. All subjects had no history of neurological illness, and had normal or corrected-to-normal vision. Informed consent was obtained as per human studies committee guidelines at Washington University School of Medicine.

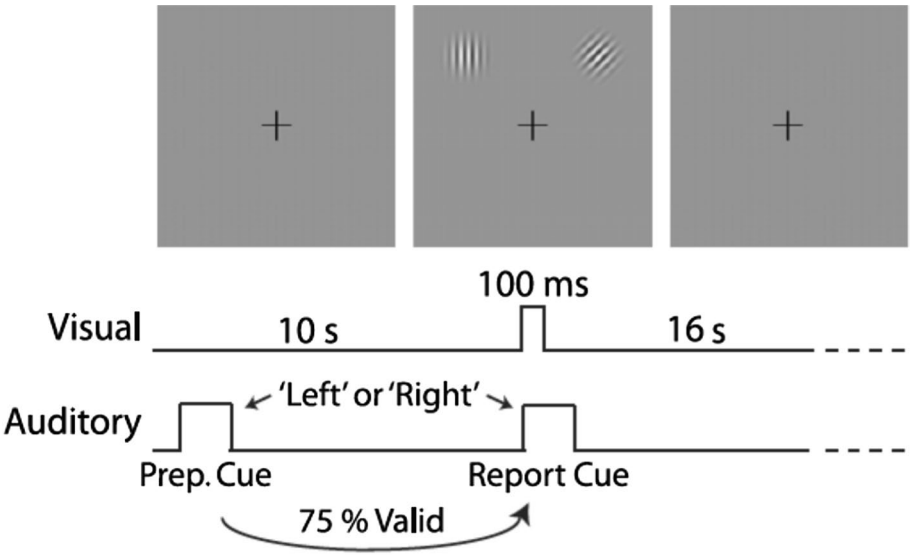

Fig. 1 Visual spatial attention paradigm. Each trial began with an auditory preparatory cue ("left" or "right") that instructed the subject to attend covertly to a location in the upper visual hemifield, either left or right of the vertical meridian, while maintaining fixation on a central crosshair. Visual stimuli appeared 10.32 s later, with 100 ms duration, at both locations, concurrent with an auditory report cue ("left" or "right"). The subject was required to indicate the orientation of the (target) stimulus at the location indicated by the report cue. To allow evoked activity to return to baseline, a long (16 s) post-target period followed, during which subjects maintained fixation on the central crosshair

Task trials began with a 500 ms auditory preparatory cue (the spoken word "left" or "right"), which directed covert attention to one of the two locations at 5° eccentricity in the upper visual hemifield, 45° clockwise or counterclockwise from the vertical meridian hemifield. Right- and left-cued trials were randomly intermixed with equal probability. Trials had target stimulus-onset asynchrony (SOA) of 6.192 (25%), 8.256 (25%), or 10.32 s (50%). To maximize the number of observations (i.e., time points) in the anticipatory, pre-target period, only the longest SOA trials were included in the present study, reflected in Fig. 1. Targets were 3.5 cycles per degree Gabor patches (0.3° Gaussian envelope SD). Subjects indicated the orientation (left tilt, vertical, right tilt) of the report-cued patch by pressing one of the three buttons. The report cue was either the same as (valid trials, 75%) or opposite to (invalid trials, 25%) the preparatory cue. Only valid trials were included in the present study. Two stimulus parameters—target contrast and difference in orientation between targets—were adjusted based on in-scanner practice sessions: for each subject, minimal values were selected such that they could still achieve approximately 70% correct valid trial performance (range 5–12% and 6–45°, respectively). Mean task performance was 70.6% correct for valid and 61.5% correct for invalid trials (chance = 33.3%), indicating that subjects used the preparatory cue to discriminate the target. Because incorrect trials occurred less frequently, including them in the analysis would have required reducing the number of correct trials to achieve balance across conditions. Therefore, incorrect trials were excluded; only correct trials were used in order to maximize the number of observations used in computing each MVAR model. Both high (50%) and low (5–12%) target contrast trials were used and not distinguished (see Undirected and Directed Functional Connectivity Analyses below for further explanation).

Eye position was monitored to ensure fixation on the crosshair. Eye movements were recorded using an ISCAN (Burlington, MA) ETL-200 system, which consisted of a video camera aimed through the back of the scanner bore and focused on the reflection of subjects' eyes in the mirror attached to the head coil. These recordings were used to confirm eye fixation during the task. Eye movements of one of the five task subjects (author CS) were not monitored.

Data acquisition

BOLD data of both Task and Rest Groups were acquired with a Siemens Allegra 3T scanner using a gradient echo sequence [repetition time (TR) = 2.065 s, echo time = 25 ms, flip angle = 90°, 32 contiguous 4 mm axial slices, 4 × 4 mm in-plane resolution]. BOLD images were motion corrected within and between scanning sessions, corrected for across-slice timing differences, resampled into 3 mm isotropic voxels, and warped into a standardized atlas space (Talairach and Tournoux 1988).

Subjects in the Task Group were recorded while performing the task in 8–12 scanning sessions, and those in the Rest Group were recorded in a single scanning session (consisting of 6–7 scans). 176 volumes were collected per task scan, and 124 per resting scan.

Region of interest creation

For each subject, BOLD data at each voxel were subjected to a general linear model using in-house software. Constant and linear terms modeled baseline and linear drift, while sine waves modeled low-frequency noise (<0.009 Hz) within each scan.

Two sets of ROIs were created for use in either a within-task analysis on Task Group subjects alone, or a between-groups analysis comparing Task and Rest Group subjects (see *Undirected and Directed Functional Connectivity Analyses* below). First, for the analysis within the Task Group, separate δ function regressors coded each time point after the preparatory cue. To generate individual-trial BOLD time series, these modeled responses of the appropriate event type were summed with the residuals from the general linear model (i.e., the remainder after subtracting modeled baseline, linear drift, and low-frequency noise) at each time point. Thus, individual-trial time series consisted of the original signal (including task-evoked responses) minus constant, linear drift, and sine wave terms. Regions Of Interest (ROIs) outside retinotopic cortex were created by voxelwise analysis of variance in each subject over the first six trial time points using the residuals from the general linear model. The ANOVA effects of interest were cue direction, target contrast, validity, performance, and time. An in-house clustering algorithm defined ROIs from the map of the main effect of cue direction. ROIs were 8-mm-radius spheres centered on map peaks with z-scores >3; spheres within 12 mm of each other were consolidated into a single ROI. To reduce inter-subject variability, ROIs were retained for subsequent analysis if they were defined in at least 6 of the 12 subject hemispheres. ROIs included the FEF (at the junction of the superior frontal sulcus and the precentral sulcus), anterior IPS (aIPS), and posterior IPS (pIPS). If a subject lacked a particular ROI, the z-score threshold was lowered to 2; if the subject still lacked the ROI, it was excluded from subsequent analysis. As a result, two subjects lacked left hemisphere aIPS and FEF. Importantly, this only affected the ROI set for the within-task analysis (see below). For the purposes of this study, bilateral FEF, aIPS, and pIPS constitute the Dorsal Attention Network (DAN) (aIPS and pIPS were merged into one IPS ROI per hemisphere for the second ROI set, see below).

ROIs inside retinotopic Visual Occipital Cortex (VOC) (V1, V2, V3, V3A, VP, and V4) were derived from a retinotopic mapping procedure in which subjects passively viewed contrast-reversing checkerboard stimuli extending along the horizontal and vertical meridians. Using a contrast of responses to the horizontal and vertical meridians, the boundaries of early retinotopic visual regions were hand drawn on flattened representations of each subject's cortex with the Caret software suite (Van Essen et al. 2001). The V3A ROI consisted of V3A voxels with responses that varied with the direction of the preparatory cue. In separate localizer scans, subjects passively viewed high-contrast (~50%) Gabor patches that flickered at 4 Hz. In 12 s blocks, a patch randomly appeared at one of the five locations (two target, two mirrored across the horizontal meridian, and one central). Voxels representing each of these locations were localized by t tests. Voxel responses to each non-central stimulus were significantly larger than to those of its mirror stimulus across the vertical meridian. Responses to the central location were significantly larger than the summed responses to all other locations. Voxel sets making up ventral (V1v, V2v, VP, V3Av) and dorsal (V1d, V2d, V3, and V3Ad) retinotopic areas were formed by the conjunction of voxels having a stimulus preference in the localizer scans and the retinotopic regions corresponding to upper and lower hemifield locations, respectively. Unlike V3A, V4 was not subdivided into upper and lower hemifield retinotopic regions, and thus contained a full representation of both hemifields.

For the analysis between Task and Rest Group subjects, ROIs were created based on leave-one-out averages of the Talairach coordinates of the ROIs that were individually defined in the procedure just described (bilateral V1v/d, V2v/d, VP, V3, V3Av/d, V4, a/pIPS, FEF). For each Task Group subject, a coordinate for each ROI in the DAN and VOC was computed as the average of the coordinates for that ROI from all Task Group subjects excluding the subject in question. Because of their proximity, one coordinate was computed for aIPS and pIPS, thus merging them into one IPS ROI for this analysis. This procedure yielded six unique sets of coordinates, one for each Task Group subject. A sphere of radius 7 mm was centered on each coordinate to yield ROIs that matched the average size across subjects of the individually defined ROIs used in the within-task analysis. Each Task Group subject was assigned the one ROI set (out of six total) that was based on the average of the other five Task Group subjects. The six ROI sets were then assigned randomly and evenly to the Rest Group subjects. Thus, the ROIs for each subject in both groups were not localized on an individual basis, but were based on the averages of five other individual localizations. This eliminated the possibility that differences between Task and Rest Groups could be attributed to a bias from having individually localized ROIs in the Task Group but not the Rest Group. Finally, as a result of this procedure, all subjects had a full set of ROIs for the analysis between Task

and Rest Groups. Only in the within-Task Group analysis did two subjects lack L FEF and aIPS, and thus a full set.

BOLD time series preprocessing

Outlier voxels were rejected based on their BOLD amplitude variability—computed either over the time course of each scan separately in the between-groups analysis, or over all correct trials in the within-task analysis—using Tukey's boxplot technique: voxels with temporal or across-trial variance greater (lower) than three times the interquartile range above (below) the 3rd (1st) quartile were considered outliers. Voxels with zero amplitude were also rejected. BOLD time series were z-normalized to have zero mean and unit variance. As with outlier rejection, normalization was performed over time for each scan separately in the between-groups analysis or over all correct trials for the within-task analysis.

Undirected and directed functional connectivity analyses

Undirected functional connectivity (UFC) was measured at the voxel-to-voxel level by the zero-lag Pearson product-moment correlation, which was computed using the *cor.test* function in the R software environment. Bivariate correlations were computed for all voxel pairs in the set of voxels constituted by the DAN and VOC ROIs. For the within-task analysis, correlations were computed across trials, yielding one UFC value for each voxel pair at each time point in the trial. This allowed for analysis of changes in UFC across the two trial periods (pre-target and post-target). It also matched the trial-based method for estimating directed functional connectivity described below. For the between-groups analysis, correlations were computed across time series: in the Task Group, time series consisted of the pre-target periods of a subject's full set of valid, correct trials concatenated together, while in the Rest Group time series consisted of a subject's concatenated resting-state scans. This yielded one UFC (correlation) value per voxel pair for each subject. Pairwise voxel UFC values were then aggregated into a summary metric to give ROI-to-ROI UFC as described below.

Directed functional connectivity (DFC) was measured at the voxel-to-voxel level using a multivariate autoregressive modeling (MVAR) approach, which is an extension of that developed by (Tang et al. 2012). The present approach differs in three important respects. First, whereas previously a separate MVAR model was estimated based on present and past BOLD values from voxels in one ROI pair at a time, here MVAR models incorporated BOLD values from all DAN and VOC ROI voxels simultaneously to achieve maximum conditionalization on latent influence in coefficient estimation. As previously mentioned, model selection was achieved using the Least Absolute Shrinkage Selection Operator, or the LASSO (Tibshirani 1996), which places a constraint on the $\ell 1$-norm of the model coefficients from each independent row of the MVAR equation, with the effect of setting most coefficient values in each row to zero. Second, whereas previously LASSO was implemented using Least Angle Regression, or LARS, here it was implemented using the more recently developed glmnet algorithm (Tibshirani et al. 2010) in the R software environment. Third, previously trials were split into two half-sets: one half-set was used to allow the LASSO to select variables for which non-zero coefficients could be estimated, while the other half-set was used to estimate model coefficients and their associated t-statistics for those selected variables alone via Ordinary Least Squares. However, a major drawback of this approach is loss of power due to halving of the observations. Thus, here variable selection and model coefficient estimation were performed simultaneously using the full set of trials with no significant testing. The presence of a non-zero model coefficient b_{ij} indicated DFC from the jth to the ith voxel conditional on all other voxels in the model.

Models were fit separately for left- and right-cued trials. The number of trials of each type was balanced within each subject to ensure equal observations for model fitting across the two types. Because by design there were many fewer incorrect than correct trials, incorporating incorrect trials would have required balancing to a much smaller number of observations and would have reduced model estimation accuracy. Therefore, only correct trials were used.

As with UFC, DFC was estimated separately for a within-task analysis on the Task Group alone and a between-groups analysis on both Task and Rest Groups. For the within-task analysis, a trial-based method followed previous studies (Bressler et al. 2008; Tang et al. 2012) in estimating DFC in a single time window (two time-point duration), with all of the trials contributing observations from that window. Trial-based estimates were obtained separately for each of the 12 time points in the trial (5 pre-target and 7 post-target), where DFC at each time point was estimated from an order-one MVAR model in which the data at that time point were predicted from data at the previous time point. Thus, the twelve time-point estimates were derived from a total of thirteen time points in each trial.

For the between-groups analysis, DFC was estimated using a sliding window approach. In Task Group subjects, the pre-target periods of all valid, correct trials were concatenated and a window of two time-point duration was slid across such that each adjacent pair of time points (save for those spanning gaps between concatenated trials) formed an observation for model fitting. In the Rest Group, the

equivalent operation was performed but by concatenating resting-state scans. This analysis was limited to the pre-target period of the task for two reasons: to set the number of observations used to estimate MVAR models to be roughly equivalent across groups, and to restrict the task-rest comparison to the portion of the task during which anticipatory attention was engaged.

ROI-to-ROI summary metrics

Both UFC and DFC were aggregated from voxel-to-voxel values to give ROI-pairwise summary metrics. For UFC, the metric was simply the average of all correlation coefficients over all voxel pairs between ROI A and ROI B, and was thus called strength per correlation, or SPC. Coefficients were Fisher z-transformed before averaging and the averages were then transformed back into r-values. Each region pair had one associated SPC value for each dimension of the data.

For DFC, we previously developed a metric called W (Tang et al. 2012), which represented the average net DFC strength from voxels in a "sending" ROI to voxels in a "receiving" ROI. W was computed by first summating the non-zero sending coefficients to each voxel in the receiving ROI, and then averaging those sums across receiving voxels. In equation form:

$$W_{A\to B} = \frac{\sum_{y=1}^{N}\left[\sum_{m=1}^{M} b_m\right]_y}{N},$$

where b_m represents non-zero coefficients from voxels in sending ROI *A* to voxels in receiving ROI *B, m* is the number of non-zero coefficients to a receiving voxel y in *B*, and *N* is the number of voxels in *B* for which $m \neq 0$. Because W involves averaging, it reflects both coefficient magnitudes and their signs (positive or negative). However, it is unclear which of these contributes more to its value.

To address this issue, we correlated W with a complementary second metric called the positive ratio, or PR, which was computed as the proportion of positively signed coefficients out of the total "received" non-zero coefficients by one ROI from another ROI. In equation form:

$$PR_{A\to B} = \frac{\sum_{m=1}^{M} \mathrm{sgn}_+(b_m)}{M}$$

where b_m represents non-zero coefficients from voxels in sending ROI *A* to voxels in receiving ROI *B, M* the total number of these coefficients, and $sgn_+(x)$ is equal to 1 when *x* is positive and 0 otherwise. Using ~10,000 observations of ROI-pairwise DFC, we found that W and PR correlated very closely, with $r = 0.79$, which corresponds to ~60% shared variance (see Supplementary Fig. 1 for corresponding scatter plot). We therefore concluded that the two measures are largely redundant, and that W mainly reflects the balance of positive and negative coefficients associated with voxels in a receiving ROI. Because a coefficient's sign is less subject to estimation error than is its magnitude, we opted to use PR as the ROI-to-ROI DFC metric. A positive model coefficient indicates future activity in a predicted voxel as being in the same direction as the past of the predicting voxel, and thus can be interpreted as indicating potentiating influence (while a negative coefficient can be interpreted as indicating opposing influence). Thus, this metric reflected the degree to which the net influence of one ROI on another was generally potentiating.

ROI-to-ROI DFC was computed in each direction between pairs of ROIs at two levels of analysis. The first level consisted of pairs of ROIs between the DAN and VOC, and the second of pairs within the DAN (i.e., between FEF and a/pIPS). Two global directions of influence could be measured at each level. Between DAN and VOC, the global top-down influence was the average DAN-to-VOC influence and vice versa for the global bottom-up influence. Within DAN, the two directed influences were simply FEF→IPS and IPS→FEF. For each level, only within-hemisphere pairs were considered in further analyses.

Statistical analysis

For the within-task analysis, repeated measures analysis of variance (ANOVA) was used to test whether UFC and DFC significantly differed according to different within-subject factors. In multiple ANOVAs (described below), factors tested included direction of functional connection (for DFC only), ROI pair, and trial period (pre- vs. post-target). Since the trial period factor reflected changes in attentional demands across the trial, only effects involving this factor were of interest. These repeated measures ANOVAs represented within-subject effects, and thus showed what was common to each subject after accounting for individual variability. For the between-groups analysis, mixed ANOVAs consisted of the between-subjects factor of condition (task vs. rest) along with within-subjects factors. ANOVA was performed using the *aov* function in the R software environment. Because the design of the between-groups analysis was unbalanced, we also computed multi-level models analogous to the mixed ANOVAs, since these are robust to unbalanced designs. These models included subject as a random-intercept effect, and were computed using the *lmer* function in the *lme4* package in R. These provided reassurance that effects indicated in the ANOVAs were genuine and not spurious due to the unbalanced design. When main effects or interactions were significant in the ANOVA, post-hoc *t* tests were performed (using the *t.test* function in the R software environment) to make specific

comparisons between levels. The *t* tests used subjects as observations, and the *p* values were corrected for multiple comparisons by false discovery rate (using the *p.adjust* function in the R software environment). Finally, to quantify correspondence of resting and task-evoked patterns of DFC, Pearson correlations were computed using the *cor.test* function in R.

A flowchart depicting the analysis steps can be found in Supplementary Fig. 2.

Results

Average BOLD trial time courses

Figure 2 shows average trial time courses (averaged across trials, voxels, and subjects) of BOLD signals recorded during task performance from FEF, IPS (averaged across a/pIPS), and VOC (averaged across all retinotopic subdivisions). More in-depth analyses of both trial-by-trial and average BOLD time courses from this dataset have been conducted previously (Sylvester et al. 2007, 2009). Here, they mainly illustrate characteristics of DAN and VOC task-evoked responses that serve as important context for our functional connectivity analyses.

First, following the preparatory auditory cue (the spoken word "left" or "right") there is a modest bilateral response in VOC and somewhat larger bilateral responses in both FEF and IPS, with a tendency for greater responses in the left hemisphere. These pre-target responses peak by the 4th or 5th frame (~6–8 s), whereupon they sustain in characteristic fashion in FEF and IPS (Corbetta and Shulman 2002), but decay toward baseline in VOC, and likely reflect mainly the endogenous processes of shifting and maintaining attention in anticipation of the target and the required motor response. Crucially, the timing of the peaks suggests that this anticipatory process becomes established well before target onset.

Second, following the presentation of the visual stimulus (indicated by the dashed line in Fig. 2)—which always consists of two stimuli, one in each of the left and right hemifields, and in which the target is indicated by a second auditory report cue (also the spoken word "left" or "right")—there are robust bilateral responses in all regions, which peak at a similar latency as the pre-target responses. These post-target responses likely reflect a mixture of visual stimulation, perceptual discrimination of the target, and attentional modulation, and, particularly in FEF and IPS, may additionally reflect motor response execution. Crucially, these responses decay to baseline by the end of the trial and therefore do not contaminate subsequent pre-target activity.

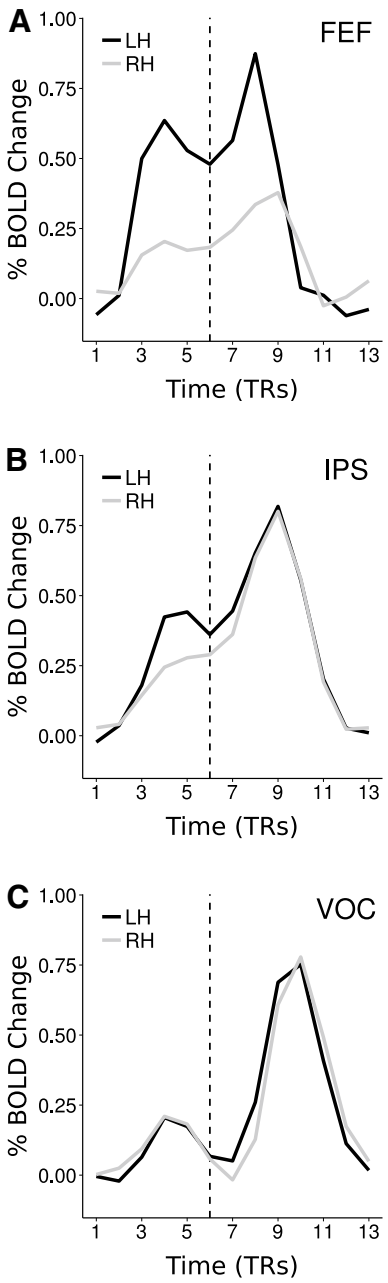

Fig. 2 BOLD trial time courses, averaged across voxels, trials, and subjects, from FEF (**a**), IPS (**b**), and VOC (**c**). The time courses serve to illustrate that (1) bilateral pre-target responses follow the preparatory cue and peak well before visual target/report cue onset (*dashed line*), and sustain in FEF and IPS while decaying in VOC, and (2) bilateral post-target responses to the visual stimulus/report cue peak at a similar latency as do pre-target responses, and decay to baseline before the beginning of the subsequent trial, ensuring that pre-target endogenous activity is uncontaminated. Note that by virtue of being averages, these time courses obscure variability across voxels, trials, and subjects, and thus give merely a coarse overview of the response characteristics of the two trial periods, with minimal insight into finer connectivity patterns throughout the trial

Resting versus task-evoked DFC and UFC

To assess the relationship between resting and task-evoked functional connectivity, we compared DFC and UFC between task and rest conditions, restricting the focus on the task to the pre-target period when functional connectivity reflected predominantly endogenous modulations underlying anticipatory attention. For DFC, we employed three-way mixed-design ANOVAs with one between-subjects factor of condition (task vs. rest) and two within-subjects factors: direction of influence (defined as above for each level) and either hemisphere (averaging across ROI pairs) or pair (within-hemisphere ROI pairs, averaging across hemispheres). For UFC, we ran analogous ANOVAs but without the direction factor. Because the condition factor was unbalanced, we also computed analogous multi-level models, which are robust to unbalanced designs. These produced consistent results (see Supplementary Tables S1–S6). Assessing FC between ROI pairs allowed for the comparison of resting and task-evoked network interactions. Assessing FC between hemispheres allowed identification of condition-specific hemispheric differences.

Resting and task-evoked global DFC and UFC patterns

Figure 3 shows the relationship between resting and anticipatory attention-related patterns of global (i.e., averaged across ROI pairs) DFC and UFC both between the DAN and VOC and within the DAN. Between DAN and VOC, DFC was directionally asymmetric. Top-down DAN→VOC influence was greater than bottom-up both during the task and at rest in both hemispheres, as indicated by a significant main effect of direction [$F(1,27)=77.99$, $p<0.0001$, $\eta^2=0.16$]. During the task, there was not only greater average global-directed influence relative to rest, as indicated by a significant main effect of condition [$F(1,27)=15.43$, $p<0.001$, $\eta^2=0.04$], but also an enhanced directional asymmetry, as indicated by a significant interaction between condition and direction [$F(1,27)=9.50$, $p=0.005$, $\eta^2=0.02$]. Post-hoc t tests showed this enhancement to consist in greater top-down DFC during the task [$t(8.47)=5.06$, $p=0.016$, $r=0.74$] with no task-rest difference in bottom-up DFC [$t(9.82)=1.14$, $p=0.282$ fdr corrected, $r=0.22$] (Fig. 3a, right panel). Thus, our results are consistent with and confirmatory for the role of top-down DAN→VOC influence in anticipatory attention while also suggesting that such top-down influence may to some extent manifest at rest.

While the directional asymmetry and its task-related enhancement pertained to both hemispheres, a significant main effect of hemisphere [$F(1,27)=8.79$, $p=0.006$, $\eta^2=0.03$] indicated a right hemisphere (RH)-dominant hemispheric asymmetry in mean bidirectional influence. As with the directional asymmetry, this hemispheric asymmetry pertained to both rest and task conditions. However, a nearly significant three-way interaction of condition,

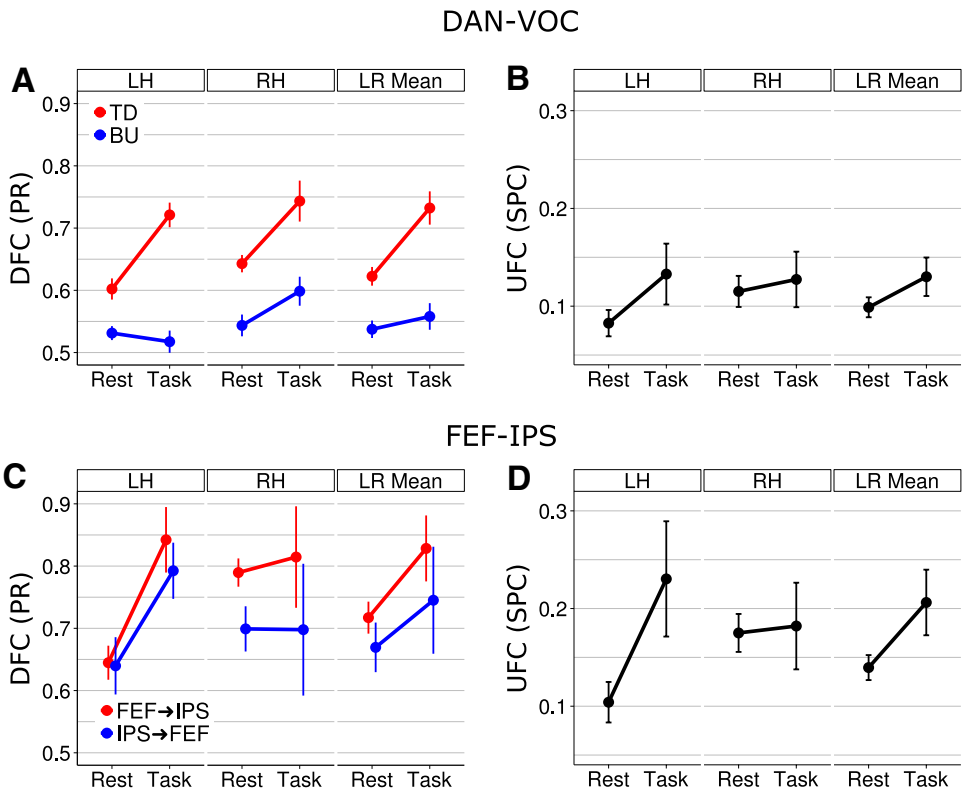

Fig. 3 Global within-hemisphere DFC and UFC in rest and task conditions, averaged across subjects, and shown for each hemisphere as well as averaged across hemispheres. Significant directional asymmetries were present in both conditions, both between the DAN and VOC (bilaterally) (**a**) and within the DAN (RH) (**c**). However, top-down DAN→VOC—but not bottom-up—influence was significantly enhanced in both hemispheres during the task relative to rest (**a**), while bidirectional FEF↔IPS influences were enhanced specifically in the LH, balancing a resting RH-dominant asymmetry (**c**). Both UFC between the DAN and VOC (**b**) and within the DAN (**d**) indicated similar task-related balancing

direction, and hemisphere [$F(1,27)=4.00$, $p=0.056$, $\eta^2=0.01$] suggested that directionally specific hemispheric asymmetries differed between rest and task conditions (Fig. 3a, left, middle panels). Indeed, post-hoc t-tests showed that during rest, top-down DFC was mildly greater in the RH than left hemisphere (LH) [$t(22)=2.46$, $p=0.045$ fdr corrected, $r=0.30$], but not during the task, while conversely bottom-up DFC was greater in the RH than LH during the task [$t(5)=4.15$, $p=0.009$ fdr corrected, $r=0.68$] but not during rest. Thus, the general RH-dominant asymmetry indicated by the main effect likely reflected these direction- and condition-specific asymmetries.

While the UFC measure of DAN-VOC interaction was consistent with DFC in that it was elevated during the task relative to rest, this condition difference was not significant (Fig. 3b, right panel). However, the interaction between condition and hemisphere was significant [$F(1,27)=11.8$, $p=0.002$, $\eta^2=0.02$]. As Fig. 3b (left, middle panels) suggests, this interaction reflected a resting RH-dominant asymmetry that became balanced during the task. While post-hoc t tests confirmed the resting asymmetry [Rest, RH vs. LH: $t(22)=7.77$, $p<0.001$ fdr corrected, $r=0.31$; Task, RH vs. LH: $t(5)=0.36$, $p=0.73$ fdr corrected, $r=0.06$], they did not, however, show significant task-rest differences in either hemisphere. Thus while DAN-VOC UFC appeared generally consistent with DFC, particularly with the top-down pattern, it appeared less sensitive in revealing attention-related enhancements of DAN-VOC interaction.

Within the DAN, effects similar to those observed between the DAN and VOC manifested for both DFC (Fig. 3c) and UFC (Fig. 3d). For DFC, these included a significant main effect of direction [$F(1,27)=4.89$, $p=0.036$, $\eta^2=0.03$], which reflected an FEF→IPS dominant directional asymmetry; a significant main effect of hemisphere [$F(1,27)=8.02$, $p=0.009$, $\eta^2=0.05$], which reflected a RH-dominant hemispheric asymmetry in mean bidirectional influence; and a main effect of condition [$F(1,27)=4.69$, $p=0.039$, $\eta^2=0.06$], which reflected greater mean bidirectional influence during the task compared to rest. Here the most striking effect was indicated by a significant condition by hemisphere interaction [$F(1,27)=7.52$, $p=0.011$, $\eta^2=0.04$], which the post-hoc t-tests confirmed reflected a resting RH-dominant asymmetry of mean bidirectional DFC [Rest RH vs. LH: $t(22)=3.19$, $p=0.005$ fdr corrected, $r=0.43$] that became balanced during the task [Task RH vs. LH: $t(5)=0.77$, $p=0.470$ fdr corrected, $r=0.22$] (Fig. 3c, left, middle panels). Thus, as Fig. 3c shows, the task-related enhancement of bidirectional DFC appeared to pertain exclusively to the LH, while in the RH bidirectional DFC remained largely unchanged. Figure 3c also suggests that the directional asymmetry indicated by the main effect of direction pertains more to the RH than LH (left, middle panels). Though the interaction between direction and hemisphere was not significant, it was near threshold, indeed suggesting a tendency for FEF→IPS dominance to occur to a larger degree in the RH than the LH, and to do so across both rest and task conditions.

Finally, UFC within the DAN mirrored DFC quite closely. As with DFC, there were significant main effects of both condition [$F(1,27)=4.88$, $p=0.036$, $\eta^2=0.11$] and hemisphere [$F(1,27)=15.95$, $p<0.001$, $\eta^2=0.08$], but more notably a significant interaction of condition and hemisphere [$F(1,27)=17.36$, $p<0.001$, $\eta^2=0.09$]. As Fig. 3d shows, and post-hoc t tests confirmed, this also reflected a resting RH-dominant asymmetry that became balanced during the task [Rest RH vs. LH: $t(22)=5.75$, $p<0.001$ fdr corrected, $r=0.46$; Task RH vs. LH: $t(5)=1.57$, $p=0.176$ fdr corrected, $r=0.26$]. Figure 3d also shows that this balancing involved selective enhancement of UFC in the LH, with no enhancement in the RH.

It is important to note here that, with respect to DFC, the differences between the task and rest groups could potentially have reflected differences in the degree of model selection between the two conditions, rather than true physiological differences. This possibility was tested via a between-groups ANOVA comparing the severity of the constraint on the rows of the MVAR models—given by the regularization parameter, λ—[see *Undirected and Directed Functional Connectivity Analyses* above and (Tang et al. 2012)] across the two conditions. This test showed no significant difference in the severity of constraint across the two conditions [$F(1,25)=0.604$, $p>0.4$]. Thus, the differences in DFC between the two groups did not reflect differences in the model selection procedure, but rather reflected true physiological differences.

In summary, both between the DAN and VOC and within the DAN, task engagement induced enhanced interregional functional interactions relative to rest. Between the DAN and VOC, this enhancement was largely specific to the top-down direction and was prominent in both hemispheres, but was slightly greater in the LH, thus acting to balance a resting RH-dominant asymmetry of top-down DFC. Within the DAN, task-related enhancement was bidirectional and specific to the LH, which had the effect of balancing a strong resting RH-dominant asymmetry in bidirectional influence between FEF and IPS. Finally, DFC was intrinsically directionally asymmetric, with top-down DAN→VOC and FEF→IPS predominating at rest, suggesting that resting global influence patterns may predispose those evoked by the task.

Resting and task-evoked cortical spatial patterns of DFC and UFC

Whereas Fig. 3 shows global DFC and UFC averaged across ROI pairs, Figs. 4 and 5 show finer spatial patterns of DFC and UFC between the DAN and VOC and their variation between rest and task. Figure 4a illustrates that for the top-down direction, the ROI-pairwise top-down influence pattern is highly consistent across conditions, and thus that the above-noted task-related enhancement of directional asymmetry did not strongly favor particular ROI pairs. A near-threshold but non-significant three-way interaction in a mixed condition X direction X pair ANOVA [$F(17,459) = 1.17$, $p > 0.05$] reflected this consistency across conditions. Figure 5a illustrates this consistency further, showing a high positive correlation [$r = 0.76$, $p < 0.001$] of top-down DFC across task and rest conditions. The enhancement of global top-down influence during the task (discussed above) is apparent here as the translation of the regression line is upward from the diagonal.

Despite this consistency between resting and task-evoked influence patterns, Figs. 4a and 5a suggest a stronger task enhancement of directional asymmetry for FEF-VOC than IPS-VOC pairs (greater upward shift in both Figs. 4a, 5a for FEF-VOC pairs). This may have driven the near-threshold three-way interaction noted above. We tested this possibility by aggregating ROI-pair DFC by DAN ROI to produce a coarse spatial factor with two levels (i.e., FEF-VOC, IPS-VOC) and running a three-way mixed ANOVA with condition and direction as the other factors. The three-way interaction also showed a trend toward significance. Thus, if enhancement of top-down influence is preferential for the FEF-VOC

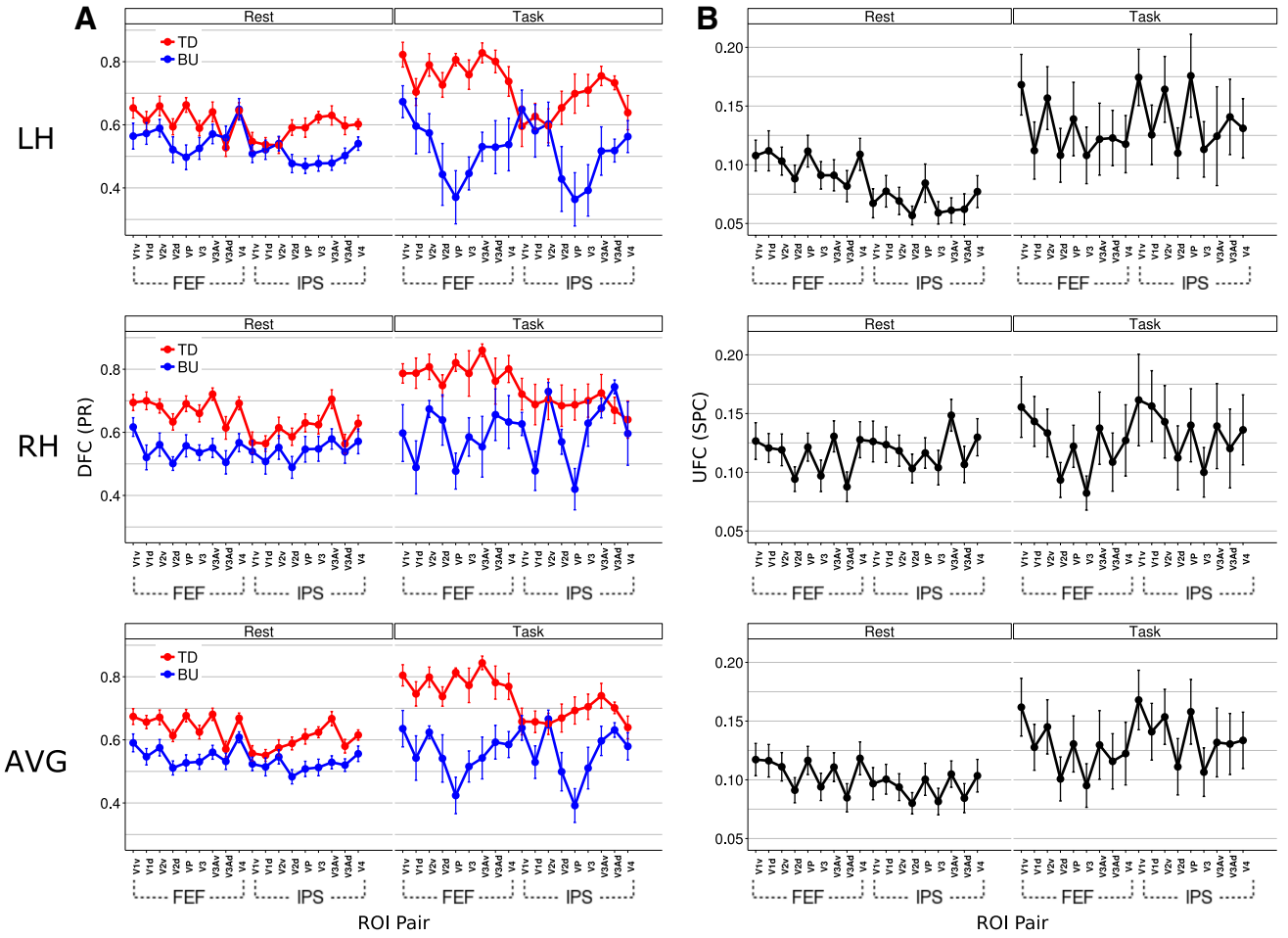

Fig. 4 Resting and task-evoked cortical spatial patterns of DFC (**a**) and UFC (**b**) across DAN-VOC ROI pairs, shown separately for LH, RH, and averaged across hemispheres (AVG). **a** The patterns of top-down DFC are remarkably similar across conditions, reflecting global task-related elevation, though they suggest greater task-related elevation for FEF→VOC than IPS→VOC DFC. Bottom-up DFC patterns are also similar across conditions, but differ notably in VP→DAN DFC. **b** UFC patterns are less similar across conditions than are DFC patterns, and suggest greater task-related elevation of IPS-VOC than FEF-VOC UFC. In both **a, b** a bias in connectivity toward ventral VOC manifests in both conditions

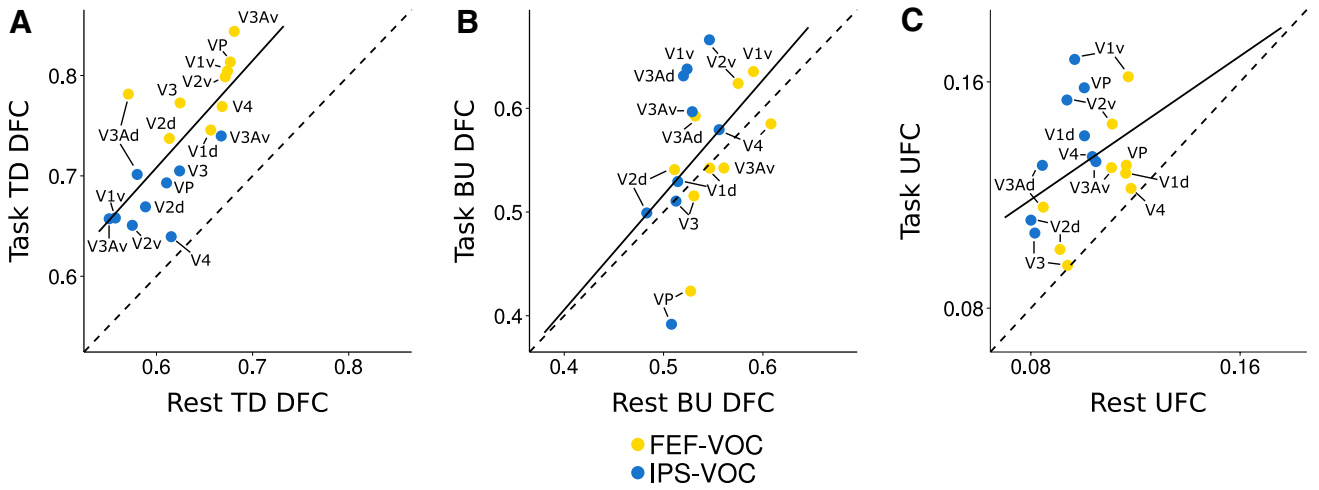

Fig. 5 Correlations of resting and task-evoked cortical spatial patterns of top-down (**a**) and bottom-up (**b**) DFC and UFC (**c**) between the DAN and VOC. Each point indicates DFC/UFC for one DAN-VOC ROI pair. Dashed diagonal lines indicate perfect correspondence between task and rest. **a** Top-down DFC displays a high task-rest correlation ($r=0.76$, $p<0.001$). The trend line is parallel to the diagonal but shifted left, indicating global task-related elevation that preserves the resting pattern, with slightly greater elevation for FEF-VOC pairs. **b** Bottom-up DFC displays lower task-rest correlation than top-down ($r=0.47$, $p<0.05$), mainly due to task-related negative shifts for FEF- and IPS-VP pairs. The trend line indicates close task-rest correspondence otherwise. **c** Task-rest correlation is lower for UFC ($r=0.39$, $p=0.52$), mainly due to greater task-related elevation for IPS-VOC than FEF-VOC pairs

component of DAN-VOC DFC, this effect may be weak, thus requiring greater statistical power to detect.

Figure 4a also suggests a bias in top-down influence from FEF toward ventral retinotopic VOC ROIs—note the zig-zag pattern, which arises due to the alternation of ventral and dorsal ROIs (excepting V4, which was not retinotopically subdivided). Surprisingly, this bias appeared to manifest not only during the task, as would be expected since covert attention was always directed toward the upper visual field, but also at rest, where though fixation was always central the covert attention was not constrained. We tested for a condition difference in top-down retinotopic bias by creating another coarse spatial factor of retinotopic subregion (aggregated dorsal vs. ventral VOC ROIs, excluding V4), and running a three-way ANOVA with condition and DAN ROI (FEF, IPS) as the other factors. A non-significant three-way interaction, together with a significant main effect of retinotopic subregion [$F(1,27)=11.72$, $p=0.002$, $\eta^2=0.03$] and a significant two-way interaction of DAN ROI with retinotopic subregion [$F(1,27)=9.437$, $p=0.005$, $\eta^2=0.01$], reflected the shared ventral bias in top-down influence from FEF across conditions suggested by Fig. 4a.

Figure 5b shows that, as with the top-down direction, the bottom-up influence was positively correlated between conditions [$r=0.47$, $p=0.049$], suggesting a similar preservation of influence pattern. In contrast to the top-down correlation, here many ROI pairs clustered around the diagonal, consistent with the absence of global modulation in bottom-up influence noted above. However, bottom-up influence from two ROI pairs—FEF-VP and IPS-VP—noticeably diverged from this pattern, moving in the negative direction during the task relative to rest, as is apparent in both Figs. 4b and 5b. This likely weakened the correlation across conditions, and additionally may have combined with greater FEF-VOC top-down DFC to drive the near-threshold three-way interaction from the condition X direction X pair ANOVA.

For the equivalent comparison of UFC (Figs. 4b, 5c), a two-way mixed ANOVA with condition and pair as factors yielded a significant two-way interaction [$F(17,459)=2.12$, $p=0.006$, $\eta^2=0.02$]. This suggested that, in contrast to DFC, UFC did change significantly more for some ROI pairs than others across conditions. A lower correlation of DAN-VOC UFC across rest and task conditions [$r=0.39$, $p=0.52$] also supported this interpretation (Fig. 5c). Despite these indications, post-hoc t tests comparing UFC during task vs. rest for each ROI pair did not reveal any significant differences ($p>0.05$, fdr corrected). However, three ROI pairs did show large effects of task-enhanced UFC: IPS-V1v ($r=0.50$), IPS-V2v ($r=0.49$), and IPS-VP ($r=0.42$). Figure 5c similarly suggests a generally greater task enhancement (greater upward shift) of UFC for IPS-VOC than FEF-VOC pairs. The significant ANOVA interaction is thus consistent with these effects. Interestingly, this contrasted with the DFC pattern, which suggested greater FEF→VOC than IPS→VOC influence during anticipatory attention.

As with DFC, Fig. 4b illustrates a similar bias in UFC toward ventral retinotopic VOC in both conditions, only

here this appeared to manifest for both DAN ROIs. We ran the same ANOVA as on DFC above (condition X DAN ROI X retinotopic subregion) to test for condition differences in this bias for UFC. Again, while the three-way interaction was not significant, the main effect of retinotopic subregion was [$F(1,27)=27.59$, $p<0.001$, $\eta^2=0.03$], and in addition there was a near-threshold effect for the two-way interaction of condition and retinotopic subregion. Together, these results reflected the same shared across-condition bias toward ventral VOC as above, but further suggested a possible mild task enhancement of this bias for UFC, which is consistent with the large-effect *t* tests noted above, each of which involved ventral VOC ROIs.

In summary, overall the comparisons of cortical spatial patterns of DFC and UFC across conditions were more remarkable for similarities than differences, suggesting that resting patterns—including retinotopic biases—were largely preserved during anticipatory attention.

Potential confound of scanner performance over time

One confound that could potentially have contributed to task-rest differences is that, while approximately half of the Rest Group ($n=12$) were recorded during the same time period as the task subjects, the remaining half ($n=11$) were recorded two years later, and as such scanner performance changes could have arisen over time and manifested as group differences in functional connectivity. To rule out this possibility, we divided the Rest Group into early ($n=12$) and late ($n=11$) subgroups, and compared them using similar mixed ANOVAs as were used to compare the task and rest groups, but replacing the 'condition' factor. That is, for UFC we ran ANOVAs with time period (early vs. late) as a between-subjects factor and hemisphere as a within-subjects factor; for DFC we ran the same ANOVAs but with the additional within-subjects factor of direction. For both between DAN-VOC and within-DAN UFC, there was neither a significant main effect of time period [DAN-VOC: $F(1,21)=0.713$, $p>0.4$; within-DAN: $F(1,21)=0.781$, $p>0.3$], nor an interaction effect of time-period X hemisphere [DAN-VOC: $F(1,21)=0.005$, $p>0.9$; within-DAN: $F(1,21)=0.956$, $p>0.3$]. For within-DAN DFC, there were also no significant effects involving the time-period factor [main effect: $F(1,21)=1.884$, $p>0.1$; time-period X direction: $F(1,21)=1.418$, $p>0.2$; time-period X hemisphere: $F(1,21)=1.825$, $p>0.1$; time-period X direction X hemisphere: $F(1,21)=0.602$, $p>0.4$]. However, for DAN-VOC DFC, there was a significant main effect of time period [$F(1,21)=12.7$, $p=0.002$], which reflected a greater mean PR in the late vs. the early group. Crucially, however, there were no significant interaction effects that depended on time period [time-period X direction: $F(1,21)=0.494$, $p>0.4$; time-period X hemisphere: $F(1,21)=0.114$, $p>0.7$; time-period X direction X hemisphere: $F(1,21)=3.132$, $p>0.1$]; thus, while there may have been an upward shift in the mean PR level in the late relative to the early group, the relationships between the two directions (top-down and bottom-up) and hemispheres did not differ between the two groups.

These results suggest that while there may have been an upward shift in the mean PR level in the late relative to the early group, the relationships between the two directions (top-down and bottom-up) and hemispheres did not differ between the two groups. Thus, the main result of a greater directional asymmetry due to elevated top-down DFC during the task relative to rest does not appear to depend on whether resting subjects were scanned contemporaneously with the task group or later on. To confirm this finally, we ran the same task-rest ANOVAs (condition X direction X hemisphere) but separately including only the early or only the late group of resting subjects. For each subgroup's ANOVA, the pattern of results was the same, where the condition X direction interaction was significant [early: $F(1,16)=9.047$, $p=0.008$; late: $F(1,15)=5.307$, $p=0.036$], and reflected elevated top-down in the task relative to rest but similar levels of bottom-up DFC between task and rest. Thus, we conclude that a confound of scanner performance due to the time period of the resting scans did not influence the main findings.

Within-task analysis of DFC and UFC

Task-evoked DFC and UFC patterns across-trial periods

In addition to the task-rest comparison, we also compared DAN-VOC and within-DAN functional connectivity patterns across the two target periods of the trial (pre- and post-target). For DFC, we computed three-way repeated measures ANOVAs with direction, trial period, and ROI pair as factors. For UFC, we ran analogous two-way ANOVAs without the direction factor. To assess functional connectivity patterns underlying anticipatory attention, we focused primarily on comparisons between the pre- and post-target periods of the trial.

Figure 6 shows whole-trial time courses of both DFC and UFC between the DAN and VOC and within the DAN. Between the DAN and VOC, the strong top-down dominant directional asymmetry reported above, which here manifested as a significant main effect of direction [$F(1,5)=61.65$, $p<0.001$, $\eta^2=0.48$], persisted across the entire trial (Fig. 6a). However, this asymmetry became enhanced following the appearance of the target, as reflected by an interaction between direction and period [$F(1,5)=26.27$, $p=0.004$, $\eta^2=0.007$]. Post-hoc *t* tests comparing mean pre- and post-target DFC revealed higher bottom-up VOC→DAN influence during the pre-target

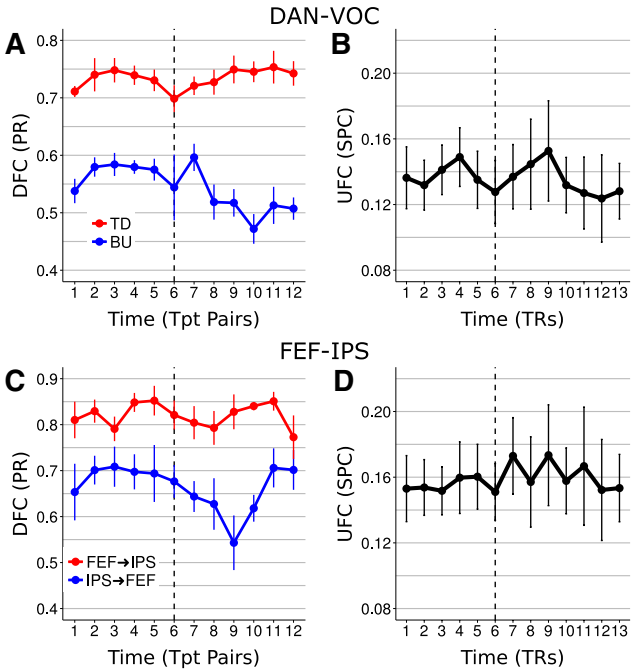

Fig. 6 Time courses of global (i.e., averaged across ROI pairs) DFC and UFC between the DAN and VOC (**a, b**) and within the DAN (**c, d**) across the trial. The dashed line indicates appearance of the target coincident with the report cue. **a** Top-down DAN→VOC DFC remained steady and dominant across the trial, while bottom-up was significantly elevated during the anticipatory period. **b** DAN-VOC UFC did not show significant change across the trial. **c** FEF→IPS DFC dominated across the trial, but bidirectional FEF↔IPS DFC was significantly elevated during the anticipatory period, and appeared to be more so for the IPS→FEF direction. **d** Within-DAN UFC did not change significantly across the trial

period [$t(5)=4.75$, $p<0.05$ fdr corrected, $r=0.48$] with no change in top-down across the trial [$t(5)=0.13$, $p=0.90$ fdr corrected, $r=0.002$]. Thus, predominant top-down influence from the DAN to VOC was not specific to the anticipatory pre-target period, but was a stable presence across the whole trial. In contrast, the higher proportion of positive bottom-up DFC in the pre- relative to post-target period suggested transient elevated information flow from VOC to the DAN during anticipatory attention.

In addition to these global directional effects, there was also a significant pair by period interaction [$F(26,130)=2.58$, $p<0.001$, $\eta^2=0.008$], indicating that mutual influence changed across the trial more for some ROI pairs than others. However, post-hoc paired t tests on pre vs. post average DFC did not show significance for any ROI pair after correction ($p>0.05$). Three ROI pairs did show large effects—aIPS-V3Av ($r=0.55$), FEF-VP ($r=0.46$), and FEF-V3 ($r=0.39$)—wherein each mutual influence between the pair members was greater during the pre-target period, suggesting stronger coupling in response to attentional demands.

Within the DAN, the FEF→IPS dominant asymmetry also persisted across the entire trial, as reflected by a main effect of direction [$F(1,5)=8.98$, $p=0.030$, $\eta^2=0.45$] (Fig. 6c). However, there was also a significant main effect of period [$F(1,5)=7.93$, $p=0.037$, $\eta^2=0.01$], underlying which was greater average bidirectional influence during the pre- relative to the post-target period. From Fig. 6c, this change in average FEF↔IPS influence appeared due in large part to a downward shift in the IPS→FEF direction following the appearance of the target, which may also have driven a near-threshold interaction of direction and period [$F(1,5)=4.19$, $p=0.096$, $\eta^2=0.006$]. Thus, while the directional asymmetry appeared stable across the trial, mutual influence between FEF and IPS was elevated during the pre- relative to the post-target period, possibly due in larger part to elevated pre-target IPS→FEF influence.

In contrast to the DFC results, for UFC, the two-way interaction of pair and period was significant between the DAN and VOC [$F(26,130)=2.14$, $p=0.003$, $\eta^2=0.002$], indicating that across-trial changes in UFC were specific to certain DAN-VOC pairs. However, post-hoc paired t tests of pre- vs. post-target UFC failed to reach significance for any ROI pair ($p>0.05$ for all pairs, fdr corrected), and there were also no strong effects, suggesting that any such changes were not robust. Moreover, the main effect of period was not significant for either the DAN-VOC or within-DAN tests, which indicated across-trial stability in their respective coupling. While this is consistent with top-down DAN→VOC DFC, DFC measures appeared to have better captured across-trial changes in global relationships within the DAN.

Effect of cue direction on contralateral versus ipsilateral DFC and UFC

Spatial selectivity of DAN and VOC anticipatory BOLD responses, in which greater activity manifests in the hemisphere contralateral than ipsilateral to the cued visual hemifield, has been shown previously (Sylvester et al. 2007, 2009). We therefore investigated whether such selectivity similarly occurs in DFC and/or UFC between the DAN and VOC or within the DAN. Because we measured DFC and UFC separately for right- and left-cued trials, we were able to create a laterality factor indicating whether measured connectivity occurred in response to an ipsilateral or contralateral attention shift. We then ran repeated measures ANOVAs on DAN-VOC or within-DAN DFC/UFC, with laterality, pair, and direction (DFC only) as factors, restricting the analysis to pre-target connectivity only. We did not find any significant effects involving laterality, suggesting that our DFC and UFC measures did not reflect spatial selectivity in the contralateral vs. ipsilateral sense.

Discussion

We measured both UFC and DFC within the DAN and between the DAN and VOC in subjects engaged in an anticipatory attention task and in subjects at rest. Our results demonstrate that, relative to rest, goal-directed attention enhanced interregional interactions, particularly for top-down influences from DAN to VOC and bidirectionally within the DAN. Counter to the RH-dominant asymmetry observed at rest, this enhancement generally favored the LH, most strikingly within the DAN, resulting in more balanced intrahemispheric connectivity strength across the hemispheres. Whereas this enhancement largely indicated long-timescale, tonic reconfiguration of resting organization spanning the entire task, within-trial fluctuation of bidirectional within-DAN and bottom-up VOC→DAN influences indicated short-timescale, phasic responses to changes in attentional demand. Both spatial patterns of connectivity and directional asymmetries corresponded closely between rest and task, suggesting a predisposing role of resting with respect to task-related directed functional organization.

Task-rest differences indicate tonic modulations of resting connectivity

The hypothesized role for the DAN in goal-driven attention has long centered on its putative top-down influence on sensory cortex (Corbetta and Shulman 2002). In demonstrating enhanced DAN→VOC DFC in the task relative to rest, our results strongly reinforce such influence as crucial, extending our previous findings (Bressler et al. 2008) and echoing others' (Vossel et al. 2012). Our findings are particularly consistent with those of Spadone et al. (2015), who also found task-induced, selective enhancement of top-down influence relative to rest. However, our results offer additional insight by demonstrating that this enhancement: (i) occurs in the absence of visual stimulation and thus reflects an endogenous, anticipatory process, and (ii) remains stable across the trial's anticipatory and passive fixation periods, which suggests that top-down modulation is a tonic process operating on the timescale of the entire task. Here, we are consistent with (Ozaki 2011), who, using a similar task and method, also reported across-trial stability in top-down influence, as well as with other reports of prolonged task-related functional connectivity between prefrontal and visual cortex (Zanto et al. 2011; Chadick and Gazzaley 2011). The similar stable nature of UFC and top-down DFC in our results suggests that functional connectivity between frontoparietal and visual cortex reflects mainly top-down processes.

As with top-down DFC, task engagement enhanced DFC bidirectionally within the DAN relative to rest, again consistent with Spadone et al. (2015). However, our results show this effect to be highly selective for the LH for both DFC and UFC, effectively balancing a strong RH-dominant resting asymmetry of FEF-IPS coupling. By contrast, top-down DAN→VOC influence was only mildly RH-dominant at rest, and thus showed a smaller balancing effect. As with top-down enhancement, the balancing effect was also tonic. These tonic effects may reflect the active maintenance of task-related cognitive processes known as task set (Sakai 2008), which may be a reconfiguration of resting organization sustained throughout the task.

Given that DAN-VOC UFC followed the within-DAN pattern, our results indicate a RH-dominant asymmetry in resting connectivity that becomes symmetric during task execution. Recent reports have found similar RH-dominant resting connectivity between frontal regions (Medvedev 2014), and within both the DAN and the ventral attention network (VAN) (Wang et al. 2014a). The VAN is known to be right lateralized both functionally (Corbetta et al. 2008; Corbetta and Shulman 2011; Vossel et al. 2012) and anatomically in regard to its underlying white matter connectivity (De Schotten et al. 2011), and to exert influence on the DAN during stimulus-driven re-orienting. Thus, the asymmetry we report here could indirectly reflect spontaneous modulation of the DAN from the RH-lateralized VAN. More generally, these network-specific effects may be manifestations of a recently reported tendency for the RH as a whole to be more bilaterally integrative compared to the LH (Gotts et al. 2013).

To our knowledge, the effects of task engagement on resting hemispheric asymmetries of UFC/DFC have not been systematically explored. Though some have reported symmetrical attention-related activation within the DAN (Shulman et al. 2010), possibly due to larger LH than RH activations that may balance a RH-dominant asymmetry (Szczepanski et al. 2010), the ROIs used in these studies were not topographically defined. More recent studies utilizing topographically mapped ROIs have shown greater spatial representation in the RH than LH in visual short-term memory (Sheremata et al. 2010) and attention (Sheremata and Silver 2015; Rosen et al. 2015), suggesting task-related RH-dominance. However, these asymmetries were of activation, not functional connectivity; it is possible that activation manifests these task-related asymmetries while connectivity does not. It should finally be noted that the balancing we report may be a result of the uniform right-handedness of our task subjects, as well as the use of a linguistic auditory cue, both of which certainly engaged the LH during motor preparation and cue processing, and may have engendered greater LH UFC/DFC. However, the question remains of why resting DAN connectivity is RH-dominant, and how this asymmetry impinges upon task-related connectivity. Thus, further research into this relationship is

warranted, especially in relation to spatial neglect, whose greater incidence following RH damage may be explained by RH-dominance in attention systems.

Phasic modulation of resting influence patterns may facilitate anticipatory attention

In contrast to top-down effects, bidirectional FEF↔IPS influence was elevated during the pre-target period relative to the ITI, implicating heightened within-DAN influence as instrumental to attentional control. This refines our previous report of unidirectional FEF→IPS dominant influence as key (Bressler et al. 2008) (this was both sustained across the trial and during rest), but runs contrary to others. Our finding that FEF→IPS influence was dominant at rest is at odds with (Ozaki 2011), who found it to be specifically evoked by anticipatory attention. Also, (Vossel et al. 2012) found only IPS→FEF influences to be modulated by attention (though see our Fig. 6c). While these discrepancies may reflect methodological differences, they may indicate that bidirectional—rather than solely unidirectional—frontoparietal influence is of true importance. This is implied by findings from electrophysiology of frontoparietal oscillatory synchronization during attention and other cognitive tasks (Buschman and Miller 2007; Siegel et al. 2008; Daitch et al. 2013). Given these discrepancies however, further research into directed frontoparietal influences underlying attention and cognition is needed.

Paralleling the phasic FEF↔IPS effect was a similar pre-target, phasic elevation of bottom-up VOC→DAN influence. Such enhanced bottom-up influence has been reported during visual perception (Wang et al. 2013; Dentico et al. 2014), but to our knowledge has not been associated with stimulus-independent anticipatory attention. This enhancement could reflect greater transmission fidelity from VOC to the frontoparietal areas that relaxes once the target stimulus disappears, a notion consistent with the putative gain enhancement of visual neurons thought to be driven by stimulus-independent, top-down influence. Independent of this speculation, these phasic effects indicate that increases in attentional demand drove greater integration between DAN and VOC components, consistent with the notion that cognitive demand induces greater integration among distributed regions via strengthening of long-range connectivity (Varela et al. 2001; Kitzbichler et al. 2011; Giessing et al. 2013; Cohen et al. 2014).

Resting influences provide context for task-evoked influences

The relevance of spontaneous activity for task-related activity has long been appreciated (Arieli et al. 1996), but has become more widely acknowledged through large-scale resting-state functional connectivity studies (Raichle 2009, 2010). Our results further this notion by finding a high correlation between resting and task-related patterns of DAN-VOC DFC, as well as the presence of resting directional asymmetries more often associated with attention (Bressler et al. 2008; Vossel et al. 2012). Echoing recent studies purporting to show a core functional connectivity architecture that remains stable across rest and many task domains (Cole et al. 2014; Krienen et al. 2014), this tight task-rest correspondence may reflect not only common anatomical and physiological constraints, but also the Hebbian shaping of resting by task-related network interactions (Lewis et al. 2009; Tambini et al. 2010; Sadaghiani and Kleinschmidt 2013). This may afford a prospective functional role for resting organization which enables minimal and efficient reconfiguration for task execution, thus constituting a cycle of mutual task-rest shaping.

Surprisingly, this task-rest correspondence applied to the retinotopic relationship between DAN and VOC, where a bias toward ventral regions manifested in both conditions. Because attention was always directed to the upper field, such a bias is expected during the task, but its presence in resting connectivity is more difficult to explain. While previous studies have shown topographic correspondence between IPS and visual cortex in anatomical white matter connectivity (Greenberg et al. 2012) and task-related functional connectivity (Lauritzen et al. 2009), and more recent studies have begun to show retinotopically determined intrinsic functional connectivity patterns within visual cortex (Gravel et al. 2014; Raemaekers et al. 2014), to our knowledge such retinotopic relationships have not been demonstrated to occur in resting connectivity between frontoparietal and visual cortex. One intriguing possibility for the presently observed bias is that it reflects a perceptual bias that occurs in healthy individuals known as pseudoneglect (Jewell and McCourt 2000). Although pseudoneglect is most commonly known as a bias toward left space in visuospatial judgment tasks (and is thus thought to reflect RH-dominance), a similar bias toward upper visual space, known as vertical pseudoneglect, has been described (Fink et al. 2001; Heber et al. 2010). Thus, it may be speculated that the resting ventral bias observed here, especially in top-down FEF→VOC DFC, underlies vertical pseudoneglect, and that because attention was always directed toward the upper field in the task, an elevation of top-down influence with no adjustment of this bias was sufficient for task performance. The obvious test of this hypothesis would be to direct attention toward the lower field. Regardless of this speculation, the preservation of retinotopic connectivity across conditions is consistent with the notion of mutual shaping of resting and task-related connectivity and influence patterns.

Attention and cognitive control

The voluntary control of visuospatial attention can be seen as a special case of the larger capability of cognitive control (Miller and Cohen 2001), the hallmark of which is flexible reconfiguration of cognitive processes in accordance with changing goals. Indeed, our results echo a set of mechanisms associated with cognitive control: top-down influence from frontoparietal to sensory cortex, frontoparietal interaction, and increased integration of cognitive networks. Our results further hint at a potentially larger role for FEF than IPS in top-down influence on VOC (Figs. 4a, 5a), echoing Spadone et al. (2015) findings. Taken with our finding that FEF→IPS influence was consistently dominant, this may reflect prefrontal cortex, of which FEF is a part (Passingham and Wise 2012), being the chief facilitator of cognitive control. Other reports that parietal cortex facilitates this control (Esterman et al. 2009) may reflect frontal-to-parietal influences. Overall, our results are consistent with the larger theme that interactions within frontoparietal networks, and between these networks and sensory cortex, are essential for cognitive control (Gerlach et al. 2014).

Comparing UFC and DFC measures

While the vast majority of functional connectivity studies have relied upon correlation of BOLD time series (i.e., UFC), our results serve to illustrate the additional insight made possible by incorporating DFC measures. Perhaps obviously, the use of DFC is necessary to test specific hypotheses regarding directed influence, as it served here to demonstrate, for example, elevated task-related top-down DAN→VOC influence relative to rest. Over and above this benefit, however, our results suggest that DFC may in addition be more sensitive than UFC in revealing modulations of functional connectivity crucial for cognition. For example, though both UFC and DFC between the DAN and VOC were consistent with each other in being elevated during the task, this elevation was significant only for DFC (Fig. 3a, b). Similarly, where UFC suggested no significant changes in either DAN-VOC or within-DAN connectivity across the trial, DFC showed that bottom-up VOC→DAN as well as bidirectional FEF↔IPS influence are significantly enhanced during the anticipatory interval of the task, and thus may crucially subserve anticipatory attending. These insights might have been missed if one employed only UFC measures, and thus argue for DFC as a crucial adjunct to UFC.

It should be noted that at least some of the differences between the UFC and DFC results may owe to differences in the way the measures were computed. In particular, the summary metric for UFC consisted of the simple average of correlation coefficients across all voxel pairs between each ROI pair (SPC), while that for DFC consisted of a weighted ratio of regression coefficients (PR). Furthermore, where correlation coefficients for voxelwise UFC were computed for each voxel pair independently, regression coefficients for voxelwise DFC were estimated conditionally on all others in the MVAR model. Thus, direct comparisons between UFC and DFC are complicated by these differences, and should be made with caution. However, the fact that both measures tend to reveal highly similar patterns (e.g., in particular, Fig. 3c, d) suggests they are by no means incommensurable. This should provide reassurance that, despite the departures from the more commonly used UFC, the DFC measure used here captures the same general connectivity phenomena as does UFC. Indeed, the additional sensitivity afforded by DFC noted above likely owes in part to its basis in conditionalized coefficient estimates, one of the main advantages of the MVAR approach (Tang et al. 2012).

Limitations

There are some limitations of note in this study. First, due to the large number of trials required for the within-task analysis, and hence long scanning time required from each task subject, the sample size in the task group was relatively small, particularly with respect to the rest group. Effects that were near statistical threshold may reflect a lack of statistical power due to this small sample size. In addition, the resultant unbalanced design poses potential problems for the mixed ANOVAs in the between-groups analysis. While this calls for some caution in interpreting the between-groups results, we provide reassurance that the task-rest differences indicated therein are genuine by computing analogous multi-level models—which are robust to unbalanced designs—as checks on the mixed ANOVAS. The results are highly consistent between the two model types (see supplementary Tables S1–S6). Therefore, we are confident that the main task-rest differences and similarities indicated by the ANOVAs are true.

Second, whereas previous studies have found that BOLD activations in DAN and VOC regions show spatial selectivity, being greater in amplitude for contralateral than ipsilateral attention (Sylvester et al. 2007, 2009), we did not find such selectivity in our connectivity measures. One possibility is that the amplitude differences reflecting spatial selectivity do not necessarily translate into differences in connectivity strength. For example, even if both DAN and VOC respond more weakly to ipsilateral orienting, their BOLD signals could remain tightly coupled, which could result in similar connectivity estimates as for when they both respond more strongly to contralateral orienting. Thus, the question of an optimal measure for spatially selective UFC and/or DFC remains an area for future inquiry.

Third, it is well-known that lag-based approaches for estimating DFC from BOLD data, such as the MVAR approach used here, have been the subject of controversy. Specifically, they appear on theoretical grounds to be susceptible to non-neural physiological confounds—namely variability in the hemodynamic response across regions and subjects (Handwerker et al. 2012), and vascular structure that dictates direction of blood flow (Webb et al. 2013)—that could cause inaccurate or even directionally reversed estimates of directed influence. Some simulation studies have appeared to confirm this proposed unsuitability. In a prominent example, Smith et al. (2011) assessed the accuracy of several different approaches for measuring both UFC and DFC from simulated BOLD data generated from a known 'ground-truth' network architecture, and found that lag-based measures performed relatively poor in recovering the known connectivity, arguing against their utility. However, Smith et al. did not include an explicit neuronal lag between simulated regions, and other simulation studies both prior and subsequent in which such lags were incorporated showed lag-based measures to perform relatively well (Roebroeck et al. 2005; Deshpande and Hu 2012; Wang et al. 2014b).

The discrepancies between these simulations underscore the larger point that, while useful, simulations are only as valid as the assumptions on which they are built, and thus cannot be taken as singularly definitive (Deshpande and Hu 2012). Understanding this, Mill et al. (Mill et al. 2016) have recently sought to validate DFC measurements using 'ground-truths' derived not from simulated data, but rather from well-established, empirically derived patterns of information flow during sensory perception vs. sensory memory. They found that lag-based Granger causality analysis on fMRI data accurately captured feedforward and feedback DFC in the appropriate contexts, thus arguing for the physiological validity of its results. The results presented in that paper are similar in that, while not supported by any explicitly known ground truth, are consistent with empirical results established using other modalities, such as microstimulation, which have demonstrated the existence and efficacy of top-down influence in visual attention (Moore and Armstrong 2003b; Moore and Fallah 2004).

In addition, while it is certainly true that lag-based DFC can produce spurious connectivity, our approach, in which DFC estimates between individual voxel pairs are aggregated by ROI pair, may provide some robustness against this, as no single estimate at the voxel level governs the patterns at the ROI pair level.

Because the physiological confounds mentioned above are stable on a short timescale, these factors do not explain the across-trial changes in DFC that we report. However, DFC patterns that were stable across the trial or differed across task and rest conditions may partly reflect non-neural effects. Nonetheless, these task-related modulations were consistent with theories of the DAN's role in top-down attention, strongly suggesting that they reflect functional processes. Furthermore, the consistency between task-related and resting DFC patterns argues against a strong effect of hemodynamic variability, though it may partially reflect neuroanatomical (Hermundstad et al. 2013) as well as non-neural constraints.

Acknowledgements TM is now at the Department of Neuroscience, Université de Montréal, Montréal, QC, H3T 1J4, Canada WT is now at the Department of Psychiatry, Basic Neuroscience Division, McLean Hospital, Belmont, MA, 02748, USA

Funding This work was supported by the National Institute of Mental Health (RO1 MH096482-01 to MC).

References

Arieli A, Sterkin A, Grinvald A, Aertsen A (1996) Dynamics of ongoing activity: explanation of the large variability in evoked cortical responses. Science 273:1868–1871. doi:10.1126/science.273.5283.1868

Baldassarre A, Lewis CM, Committeri G et al (2012) Individual variability in functional connectivity predicts performance of a perceptual task. Proc Natl Acad Sci 109:3516–3521. doi:10.1073/pnas.1113148109

Baldassarre A, Ramsey L, Hacker CL et al (2014) Large-scale changes in network interactions as a physiological signature of spatial neglect. Brain. doi:10.1093/brain/awu297

Bressler SL, Tang W, Sylvester CM et al (2008) Top-down control of human visual cortex by frontal and parietal cortex in anticipatory visual spatial attention. J Neurosci 28:10056–10061. doi:10.1523/JNEUROSCI.1776-08.2008

Buschman TJ, Miller EK (2007) Top-down versus bottom-up control of attention in the prefrontal and posterior parietal cortices. Science 315:1860–1862. doi:10.1126/science.1138071

Capotosto P, Babiloni C, Romani GL, Corbetta M (2009) Frontoparietal cortex controls spatial attention through modulation of anticipatory alpha rhythms. J Neurosci 29:5863–5872. doi:10.1523/JNEUROSCI.0539-09.2009

Capotosto P, Babiloni C, Romani GL, Corbetta M (2012) Differential contribution of right and left parietal cortex to the control of spatial attention: a simultaneous EEG-rTMS study. Cereb Cortex 22:446–454. doi:10.1093/cercor/bhr127

Carrasco M (2011) Visual attention: the past 25 years. Vision Res 51:1484–1525. doi:10.1016/j.visres.2011.04.012

Chadick JZ, Gazzaley A (2011) Differential coupling of visual cortex with default or frontal-parietal network based on goals. Nat Neurosci 14:830–832. doi:10.1038/nn.2823

Cohen JR, Sreenivasan KK, D'esposito M (2014) Correspondence between stimulus encoding- and maintenance-related neural processes underlies successful working memory. Cereb Cortex 24:593–599. doi:10.1093/cercor/bhs339

Cole MW, Bassett DS, Power JD et al (2014) Intrinsic and task-evoked network architectures of the human brain. Neuron 83:238–251. doi:10.1016/j.neuron.2014.05.014

Corbetta M, Shulman GL (2002) Control of goal-directed and stimulus-driven attention in the brain. Nat Rev Neurosci 3:201–215. doi:10.1038/nrn755

Corbetta M, Shulman GL (2011) Spatial neglect and attention networks. Annu Rev Neurosci 34:569–599. doi:10.1146/annurev-neuro-061010-113731

Corbetta M, Patel G, Shulman GL (2008) The reorienting system of the human brain: from environment to theory of mind. Neuron 58:306–324. doi:10.1016/j.neuron.2008.04.017

Daitch AL, Sharma M, Roland JL et al (2013) Frequency-specific mechanism links human brain networks for spatial attention. Proc Natl Acad Sci 110:19585–19590. doi:10.1073/pnas.1307947110

De Graaf TA, Jacobs C, Roebroeck A, Sack AT (2009) FMRI effective connectivity and TMS chronometry: complementary accounts of causality in the visuospatial judgment network. PLoS ONE 4:e8307–e8311. doi:10.1371/journal.pone.0008307

De Graaf TA, Roebroeck A, Goebel R, Sack AT (2010) Brain network dynamics underlying visuospatial judgment: an FMRI connectivity study. J Cogn Neurosci 22:2012–2026. doi:10.1162/jocn.2009.21345

De Schotten MT, Dell'acqua F, Forkel SJ et al (2011) A lateralized brain network for visuospatial attention. Nat Neurosci 14:1245–1246. doi:10.1038/nn.2905

Dentico D, Cheung BL, Chang J-Y et al (2014) Reversal of cortical information flow during visual imagery as compared to visual perception. NeuroImage 100:237–243. doi:10.1016/j.neuroimage.2014.05.081

Deshpande G, Hu X (2012) Investigating effective brain connectivity from fMRI data: past findings and current issues with reference to Granger causality analysis. Brain Conn 2:235–245. doi:10.1089/brain.2012.0091

Eriksen CW, Hoffman JE (1972) Temporal and spatial characteristics of selective encoding from visual displays. Percept Psychophys. doi:10.3758/BF03212870

Esterman M, Chiu Y-C, Tamber-Rosenau BJ, Yantis S (2009) Decoding cognitive control in human parietal cortex. Proc Natl Acad Sci USA 106:17974–17979. doi:10.1073/pnas.0903593106

Fink GR, Marshall JC, Weiss PH, Zilles K (2001) The neural basis of vertical and horizontal line bisection judgments: an fMRI study of normal volunteers. NeuroImage 14:S59–67. doi:10.1006/nimg.2001.0819

Fox M, Corbetta M, Snyder A et al (2006) Spontaneous neuronal activity distinguishes human dorsal and ventral attention systems. Proc Natl Acad Sci 103:10046

Fox MD, Snyder AZ, Vincent JL, Raichle ME (2007) Intrinsic Fluctuations within cortical systems account for intertrial variability in human behavior. Neuron 56:171–184. doi:10.1016/j.neuron.2007.08.023

Gerlach KD, Spreng RN, Madore KP, Schacter DL (2014) Future planning: default network activity couples with frontoparietal control network and reward-processing regions during process and outcome simulations. Soc Cogn Affect Neurosci 9:1942–1951. doi:10.1093/scan/nsu001

Giessing C, Thiel CM, Alexander-Bloch AF et al (2013) Human brain functional network changes associated with enhanced and impaired attentional task performance. J Neurosci 33:5903–5914. doi:10.1523/JNEUROSCI.4854-12.2013

Gotts SJ, Jo HJ, Wallace GL et al (2013) Two distinct forms of functional lateralization in the human brain. Proc Natl Acad Sci 110:E3435–E3444. doi:10.1073/pnas.1302581110

Gravel N, Harvey B, Nordhjem B, Haak KV (2014) Cortical connective field estimates from resting state fMRI activity. Front Neurosci. doi:10.3389/fnins.2014.00339/abstract

Greenberg AS, Verstynen T, Chiu Y-C et al (2012) Visuotopic cortical connectivity underlying attention revealed with white-matter tractography. J Neurosci 32:2773–2782. doi:10.1523/JNEUROSCI.5419-11.2012

Handwerker DA, Gonzalez-Castillo J, D'esposito M, Bandettini PA (2012) The continuing challenge of understanding and modeling hemodynamic variation in fMRI. NeuroImage 62:1017–1023. doi:10.1016/j.neuroimage.2012.02.015

He BJ, Snyder AZ, Vincent JL et al (2007) Breakdown of functional connectivity in frontoparietal networks underlies behavioral deficits in spatial neglect. Neuron 53:905–918. doi:10.1016/j.neuron.2007.02.013

Heber IA, Siebertz S, Wolter M et al (2010) Horizontal and vertical pseudoneglect in peri- and extrapersonal space. Brain Cogn 73:160–166. doi:10.1016/j.bandc.2010.04.006

Hermundstad AM, Bassett DS, Brown KS et al (2013) Structural foundations of resting-state and task-based functional connectivity in the human brain. Proc Natl Acad Sci 110:6169–6174. doi:10.1073/pnas.1219562110

Hopfinger JB, Buonocore MH, Mangun GR (2000) The neural mechanisms of top-down attentional control. Nat Neurosci 3:284–291. doi:10.1038/72999

Jewell G, McCourt ME (2000) Pseudoneglect: a review and meta-analysis of performance factors in line bisection tasks. Neuropsychologia 38:93–110

Kastner S, Pinsk MA, De Weerd P et al (1999) Increased activity in human visual cortex during directed attention in the absence of visual stimulation. Neuron 22:751–761

Kitzbichler MG, Henson RNA, Smith ML et al (2011) Cognitive effort drives workspace configuration of human brain functional networks. J Neurosci 31:8259–8270. doi:10.1523/JNEUROSCI.0440-11.2011

Krienen FM, Yeo BTT, Buckner RL (2014) Reconfigurable task-dependent functional coupling modes cluster around a core functional architecture. Philos Trans R Soc B. doi:10.1098/rstb.2013.0526

Lauritzen TZ, D'esposito M, Heeger DJ, Silver MA (2009) Top-down flow of visual spatial attention signals from parietal to occipital cortex. J Vis 9:18–18. doi:10.1167/9.13.18

Lewis CM, Baldassarre A, Committeri G et al (2009) Learning sculpts the spontaneous activity of the resting human brain. Proc Natl Acad Sci USA 106:17558–17563. doi:10.1073/pnas.0902455106

Marshall TR, O'Shea J, Jensen O, Bergmann TO (2015) Frontal eye fields control attentional modulation of alpha and gamma oscillations in contralateral occipitoparietal cortex. J Neurosci 35:1638–1647. doi:10.1523/JNEUROSCI.3116-14.2015

Medvedev AV (2014) Does the resting state connectivity have hemispheric asymmetry? A near-infrared spectroscopy study. NeuroImage 85:400–407. doi:10.1016/j.neuroimage.2013.05.092

Mill RD, Bagic A, Bostan A et al (2016) Empirical validation of directed functional connectivity. NeuroImage. doi:10.1016/j.neuroimage.2016.11.037

Miller EK, Cohen JD (2001) An integrative theory of prefrontal cortex function. Annu Rev Neurosci 24:167–202. doi:10.1146/annurev.neuro.24.1.167

Moore T, Armstrong KM (2003a) Selective gating of visual signals by microstimulation of frontal cortex. Nature 421:370–373. doi:10.1038/nature01341

Moore T, Armstrong KM (2003b) Selective gating of visual signals by microstimulation of frontal cortex. Nature 421:370–373. doi:10.1038/nature01341

Moore T, Fallah M (2004) Microstimulation of the frontal eye field and its effects on covert spatial attention. J Neurophysiol 91:152–162. doi:10.1152/jn.00741.2002

Ozaki TJ (2011) Frontal-to-parietal top-down causal streams along the dorsal attention network exclusively mediate voluntary orienting of attention. PLoS ONE 6:e20079. doi:10.1371/journal.pone.0020079.s005

Passingham RE, Wise SP (2012) The neurobiology of the prefrontal cortex: anatomy, evolution, and the origin of insight Oxford University Press

Posner MI (1980) Orienting of attention. Q J Exp Psychol. doi:10.1080/00335558008248231

Raemaekers M, Schellekens W, van Wezel RJA et al (2014) Patterns of resting state connectivity in human primary visual cortical areas: a 7 T fMRI study. NeuroImage 84:911–921. doi:10.1016/j.neuroimage.2013.09.060

Raichle ME (2009) A brief history of human brain mapping. Trends Neurosci 32:118–126. doi:10.1016/j.tins.2008.11.001

Raichle ME (2010) Two views of brain function. Trends Cogn Sci 14:180–190. doi:10.1016/j.tics.2010.01.008

Roebroeck A, Formisano E, Goebel R (2005) Mapping directed influence over the brain using Granger causality and fMRI. NeuroImage 25:230–242. doi:10.1016/j.neuroimage.2004.11.017

Rosen ML, Stern CE, Michalka SW et al (2015) Cognitive control network contributions to memory-guided visual attention. Cerebral Cortex. doi:10.1093/cercor/bhv028

Ruff CC, Blankenburg F, Bjoertomt O et al (2006) Concurrent TMS-fMRI and psychophysics reveal frontal influences on human retinotopic visual cortex. Curr Biol 16:1479–1488. doi:10.1016/j.cub.2006.06.057

Sadaghiani S, Kleinschmidt A (2013) Functional interactions between intrinsic brain activity and behavior. NeuroImage 80:379–386. doi:10.1016/j.neuroimage.2013.04.100

Sadaghiani S, Hesselmann G, Friston KJ, Kleinschmidt A (2010) The relation of ongoing brain activity, evoked neural responses, and cognition. Front Syst Neurosci 4:20. doi:10.3389/fnsys.2010.00020

Sakai K (2008) Task set and prefrontal cortex. Annu Rev Neurosci 31:219–245. doi:10.1146/annurev.neuro.31.060407.125642

Sheremata SL, Silver MA (2015) Hemisphere-dependent attentional modulation of human parietal visual field representations. J Neurosci 35:508–517. doi:10.1523/JNEUROSCI.2378-14.2015

Sheremata SL, Bettencourt KC, Somers DC (2010) Hemispheric asymmetry in visuotopic posterior parietal cortex emerges with visual short-term memory load. J Neurosci 30:12581–12588. doi:10.1523/JNEUROSCI.2689-10.2010

Shulman GL, Pope DLW, Astafiev SV et al (2010) Right hemisphere dominance during spatial selective attention and target detection occurs outside the dorsal frontoparietal network. J Neurosci 30:3640–3651. doi:10.1523/JNEUROSCI.4085-09.2010

Siegel M, Donner TH, Oostenveld R et al (2008) Neuronal synchronization along the dorsal visual pathway reflects the focus of spatial attention. Neuron 60:709–719. doi:10.1016/j.neuron.2008.09.010

Silver MA, Ress D, Heeger DJ (2007) Neural correlates of sustained spatial attention in human early visual cortex. J Neurophysiol 97:229–237. doi:10.1152/jn.00677.2006

Spadone S, Penna Della S, Sestieri C et al (2015) Dynamic reorganization of human resting-state networks during visuospatial attention. Proc Natl Acad Sci 112:8112–8117. doi:10.1073/pnas.1415439112

Sylvester CM, Shulman GL, Jack AI, Corbetta M (2007) Asymmetry of anticipatory activity in visual cortex predicts the locus of attention and perception. J Neurosci 27:14424–14433. doi:10.1523/JNEUROSCI.3759-07.2007

Sylvester CM, Shulman GL, Jack AI, Corbetta M (2009) Anticipatory and stimulus-evoked blood oxygenation level-dependent modulations related to spatial attention reflect a common additive signal. J Neurosci 29:10671–10682. doi:10.1523/JNEUROSCI.1141-09.2009

Szczepanski SM, Konen CS, Kastner S (2010) Mechanisms of spatial attention control in frontal and parietal cortex. J Neurosci 30:148–160. doi:10.1523/JNEUROSCI.3862-09.2010

Talairach J, Tournoux P (1988) Co-planar stereotaxic atlas of the human brain. Thieme, New York

Tambini A, Ketz N, Davachi L (2010) Enhanced brain correlations during rest are related to memory for recent experiences. Neuron 65:280–290. doi:10.1016/j.neuron.2010.01.001

Tang W, Bressler SL, Sylvester CM et al (2012) Measuring granger causality between cortical regions from voxelwise fMRI BOLD signals with LASSO. PLoS Comput Biol 8:e1002513. doi:10.1371/journal.pcbi.1002513

Tibshirani R (1996) Regression shrinkage and selection via the Lasso. J R Statis Soc Series B (Methodological) 58:267–288. doi:10.2307/2346178?ref=no-x-route:827378b2d42612d9f2f37b9441c4f3db

Tibshirani R, Hastie T, Friedman J (2010) Regularization paths for generalized linear models via coordinate descent. J Stat Softw 33(1):1–22

Van Essen DC, Drury HA, Dickson J et al (2001) An integrated software suite for surface-based analyses of cerebral cortex. J Am Med Inform Assoc 8:443–459

Varela F, Lachaux JP, Rodriguez E, Martinerie J (2001) The brainweb: phase synchronization and large-scale integration. Nat Rev Neurosci 2:229–239. doi:10.1038/35067550

Vossel S, Weidner R, Driver J et al (2012) Deconstructing the architecture of dorsal and ventral attention systems with dynamic causal modeling. J Neurosci 32:10637–10648. doi:10.1523/JNEUROSCI.0414-12.2012

Wang M, Arteaga D, He BJ (2013) Brain mechanisms for simple perception and bistable perception. Proc Natl Acad Sci 110(35):E3350–E3359

Wang D, Buckner RL, Liu H (2014a) Functional specialization in the human brain estimated by intrinsic hemispheric interaction. J Neurosci 34:12341–12352. doi:10.1523/JNEUROSCI.0787-14.2014

Wang HE, Bénar CG, Quilichini PP (2014b) A systematic framework for functional connectivity measures. Front Sci 8:1–22. doi:10.3389/fnins.2014.00405/abstract

Webb JT, Ferguson MA, Nielsen JA, Anderson JS (2013) BOLD granger causality reflects vascular anatomy. PLoS ONE 8:e84279. doi:10.1371/journal.pone.0084279.s001

Zanto TP, Rubens MT, Thangavel A, Gazzaley A (2011) Causal role of the prefrontal cortex in top-down modulation of visual processing and working memory. Nat Neurosci 14:656–661. doi:10.1038/nn.2773